

Generation of methane in the Earth's mantle: *In situ* high pressure–temperature measurements of carbonate reduction

Henry P. Scott^{*†}, Russell J. Hemley[‡], Ho-kwang Mao[‡], Dudley R. Herschbach[§], Laurence E. Fried[¶], W. Michael Howard[¶], and Sorin Bastea^{||}

^{*}Department of Physics and Astronomy, Indiana University, South Bend, IN 46634; [‡]Geophysical Laboratory, Carnegie Institution of Washington, 5251 Broad Branch Road NW, Washington, DC 20015; [§]Department of Chemistry and Chemical Biology, Harvard University, Cambridge, MA 02138; and [¶]Chemistry and Materials Science Directorate and ^{||}Physics and Advanced Technologies Directorate, Lawrence Livermore National Laboratory, Livermore, CA 94550

Contributed by Russell J. Hemley, August 12, 2004

We present *in situ* observations of hydrocarbon formation via carbonate reduction at upper mantle pressures and temperatures. Methane was formed from FeO, CaCO₃-calcite, and water at pressures between 5 and 11 GPa and temperatures ranging from 500°C to 1,500°C. The results are shown to be consistent with multiphase thermodynamic calculations based on the statistical mechanics of soft particle mixtures. The study demonstrates the existence of abiogenic pathways for the formation of hydrocarbons in the Earth's interior and suggests that the hydrocarbon budget of the bulk Earth may be larger than conventionally assumed.

Understanding the speciation of carbon at the high pressures and temperatures that prevail within the Earth has a long and controversial history. It is well known that terrestrial carbon exists in several forms: native, oxidized, and reduced in a wide variety of hydrocarbons. This complexity is demonstrated by many examples: diamonds in kimberlite formations; graphite in metamorphic rocks; CO₂ emission from volcanoes; ubiquitous carbonate minerals in the crust; methane hydrates on and beneath the ocean floor; and petroleum reservoirs in sedimentary basins. Of particular interest are the stability and formation of reduced species such as methane and heavier hydrocarbons. The stability, formation, and occurrence of methane under low-pressure conditions of the Earth's crust are well established. Recently, methane and C₂-C₄ alkanes have been documented to occur in many locations for which isotopic evidence points to an abiogenic origin (1, 2). Furthermore, it has been shown that nickel-iron alloys can catalyze the formation of CH₄ from bicarbonate (3), and that a variety of transition metal-bearing minerals can catalyze Fischer-Tropsch-type formation of hydrocarbons at conditions relevant to the upper crust (4, 5). Yet the evidence is considered to rule out a globally significant abiogenic source of hydrocarbons (2), and hydrothermal experiments suggest that with the exception of methane a vapor phase is required for the formation of heavier hydrocarbons (5). In contrast, theoretical calculations and experimental data have been presented in support of a persistent assertion that petroleum originates chiefly through abiogenic processes at the high pressures and temperatures found <100 km (6). The experiments, extending to 5 GPa and 1,500°C, involved mass spectroscopic analysis of quenched samples and found methane and smaller amounts of C₂-C₆ hydrocarbons. We report here *in situ* high pressure and temperature experiments to show that methane readily forms by reduction of carbonate under conditions typical for the Earth's upper mantle. The results may have significant implications for the hydrocarbon budget at depth in the planet.

Many factors are known to control the stability of carbon-bearing phases in the C-O-H system, including pressure, temperature, C/H ratio, and oxidation state, and it has long been appreciated that the relevant species in this system are C, O₂, H₂, CO, CO₂, CH₄, and H₂O (7). At low pressures this system is well

understood, and available thermodynamic databases can accurately predict phase stability. For example, studies of the C-O-H system in relation to crustal fluids and fluid inclusions have been carried out by using well established techniques (7, 8). Notably, theoretical modeling is both thermodynamically and observationally consistent at pressures <≈1 GPa (e.g., ref. 9) and can satisfactorily treat organic species (10). Previous experimental and theoretical work has shown that methane may be an important fluid phase at pressures of up to 1 GPa and low oxygen fugacities, and that methane may be the dominant C-bearing fluid phase at substantially reducing conditions (e.g., ref. 8). Furthermore, it has been shown that meteorite hydrocarbons can be formed by the thermal decomposition of FeCO₃-siderite at low pressure (11). Thermodynamic calculations can be performed at higher pressures (12), but the system is poorly constrained by experimental work under the high-pressure conditions of the upper mantle (13). The importance of pressure is straightforward as it increases by ≈1 GPa (10 kbar) for every 30 km of depth in the Earth. Kimberlite eruptions, for example, typically come from depths near 150 km (5 GPa). Higher-pressure work has been completed on the effects of various species in the C-O-H system on the melt characteristics of mantle minerals (14, 15), but these results do not directly assess the stability of carbon-bearing phases.

Methods

We have conducted *in situ* high-pressure and temperature experiments specifically designed to detect methane formation under geologically relevant conditions for the Earth's upper mantle. Starting materials were natural CaCO₃-calcite, FeO-wüstite, and distilled H₂O. Experiments were conducted by using diamond anvil cell (DAC) techniques: simultaneous high-pressure and high-temperature conditions were produced by both resistive (16) ($T < 600^{\circ}\text{C}$) and laser heating ($T > 1,000^{\circ}\text{C}$) methods. We used three different laser heating systems, including both single- and double-sided and both CO₂ and Nd-YLF lasers (17, 18). DACs with anvil culets ranging between 350 and 700 μm in diameter were used. Sample chambers were constructed by drilling a hole ≈70% of the culet diameter into an initially 260-μm-thick spring steel foil, which was used as a gasket material; the gaskets were preindented before drilling to a thickness of ≈60 μm. Pressure was measured by use of the ruby fluorescence technique (19). CO₂ and double-sided Nd-YLF laser heating experiments and Raman scattering and optical microscopy analyses were performed at the Geophysical Laboratory (17, 18). Pyrometry was used to determine sample temperature in selected runs. The x-ray measurements and

Freely available online through the PNAS open access option.

[†]To whom correspondence should be addressed. E-mail: hpscott@iusb.edu.

© 2004 by The National Academy of Sciences of the USA

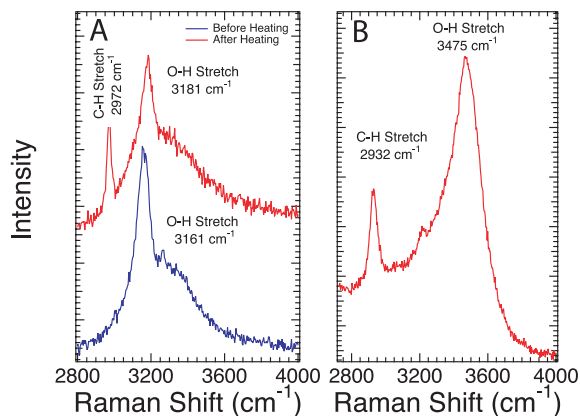


Fig. 1. Typical Raman spectra from the heating of FeO, calcite, and water near 5 GPa. The broad O-H stretching vibration of ice VII or liquid water near $3,200\text{ cm}^{-1}$ is ubiquitous in these H_2O -rich samples. (A) Raman spectrum produced by heating FeO, calcite, and water to $1,500^\circ\text{C}$ at 5.7 GPa. In isolated regions methane is the dominant Raman-active component. (B) A spectrum produced after resistively heating to 600°C and a decrease in pressure to ≈ 2 GPa; the production of methane is clearly indicated by the C-H stretching vibration at $2,932\text{ cm}^{-1}$.

double-sided Nd-YLF laser heating were performed at the High Pressure Collaborative Access Team facilities of the Advanced Photon Source, Argonne National Laboratory, Argonne, CA.

In situ analyses were made by a combination of Raman spectroscopy, synchrotron x-ray diffraction, and optical microscopy. *In situ* Raman spectroscopy proved essential because of its high sensitivity for the C-H stretching vibrations diagnostic of molecular species; it was also useful for examining amorphous or poorly crystalline phases. The synchrotron x-ray diffraction provided a means to identify crystalline phases and help determine the reactions. Both techniques allowed precise spatial resolution for probing 5- to $10\text{-}\mu\text{m}$ -diameter regions of the sample chamber, which was of particular importance for these experiments because of the heterogeneous nature of the samples.

Results

Representative Raman spectra exhibiting the presence of bulk methane from two experiments are shown in Fig. 1. Both spectra are dominated by the broad O-H stretching vibration of H_2O , but clearly indicate the presence of a hydrocarbon species with a C-H stretching vibration near $2,950\text{ cm}^{-1}$. For both experiments, a molar ratio of 8:1 (FeO/calcite), excess H_2O , and a mean grain size of $\approx 1\text{ }\mu\text{m}$ were used for starting material. For example, as seen in Fig. 1A, hydrocarbon-rich regions were found after laser heating at $\approx 1,500^\circ\text{C}$ at 5.7 GPa. The hydrocarbon was clearly identified as methane based on the sharp band at $2,972\text{ cm}^{-1}$, matching the position of bulk methane at this pressure (20). The broad feature near $3,200\text{ cm}^{-1}$ is caused by O-H stretching in ice VII (21). This sample exhibited considerable heterogeneity; Raman measurements of laser-heated experiments were typically challenging because after heating the samples were fine-grained and fluorescent, and a layer of opaque material across the diamond surface often obscured the interior of the sample chamber from optical measurements. It is important to note that the diamond anvils did not show evidence of reaction with the sample material.

We have found that the high temperatures of laser heating are not necessary for methane formation. The spectrum in Fig. 1B was collected *in situ* at 600°C . Resistive heating was initiated at 5.1 GPa, and the temperature was ramped at a rate of 50° per min. The O-H stretching vibration at $3,475\text{ cm}^{-1}$ is caused by the liquid phase of H_2O . There may be a low-intensity feature near

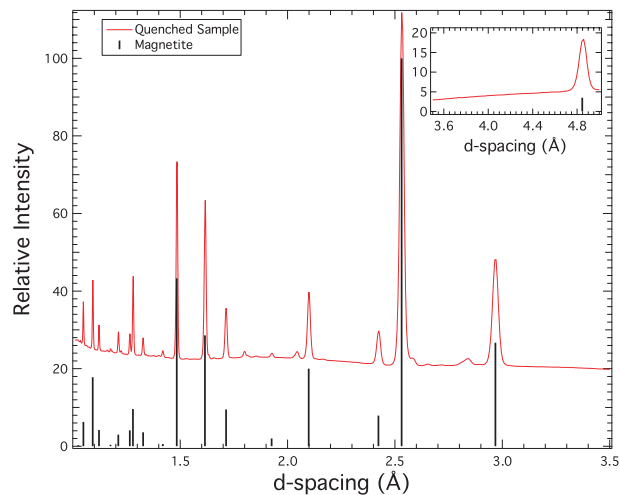
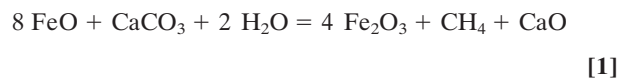


Fig. 2. X-ray diffraction pattern for temperature and pressure quenched sample after external heating to 600°C at 5 GPa. Fe_3O_4 -magnetite dominates the spectrum; weak lines suggest a Ca-Fe oxide.

$3,200\text{ cm}^{-1}$, but it was not reproducible and we do not make an assignment at this time. The C-H stretching band of methane was apparent by 500°C and became very strong and ubiquitous in the sample chamber by 600°C . Indeed, it appeared that the amount of methane is larger in the lower-temperature experiments.

In situ synchrotron x-ray diffraction was used to constrain the principal reaction. The possible reactions include the following:



and

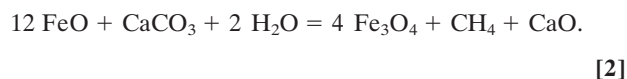


Fig. 2 shows powder diffraction from a sample after pressure and temperature quench. The 1D pattern is dominated by Fe_3O_4 -magnetite, but weak diffraction lines of another, likely Ca-bearing phase are present as well. Notably, on the 2D detector image from which this pattern was derived, it is clear that these lines are from spotty diffraction rings; this finding indicates a coarsely crystalline nature, and phase identification is accordingly difficult. The presence of abundant magnetite strongly favors a reaction such as Eq. 2, but the diffraction data are inconsistent with a chemically simple phase such as CaO or $\text{Ca}(\text{OH})_2$ and suggest a calcium ferrite chemistry such as CaFe_5O_7 , CaFe_4O_7 , or CaFe_2O_4 .

Additional information was obtained from *in situ* optical microscopy carried out in conjunction with the spectroscopy and diffraction. Indeed, detailed examination of the samples as a function of pressure and temperature revealed characteristic changes indicative of methane formation. Most notable was the extensive bubble formation, shown in Fig. 3, that accompanied decompression of the samples at room temperature. Despite the low density of bubbles, micro-Raman measurements indicate that they are predominantly methane. Fig. 3 shows a spectrum from a bubble collected after decompressing a sample that was heated at 5.7 GPa; a very weak feature attributable to methane was observed. Also significant is the fact that none of our experiments at pressures >10 GPa have been successful in producing quality Raman spectra. However, all experiments have displayed bubble growth on decompression to pressures <1 GPa. Therefore, the formation of methane may be widespread

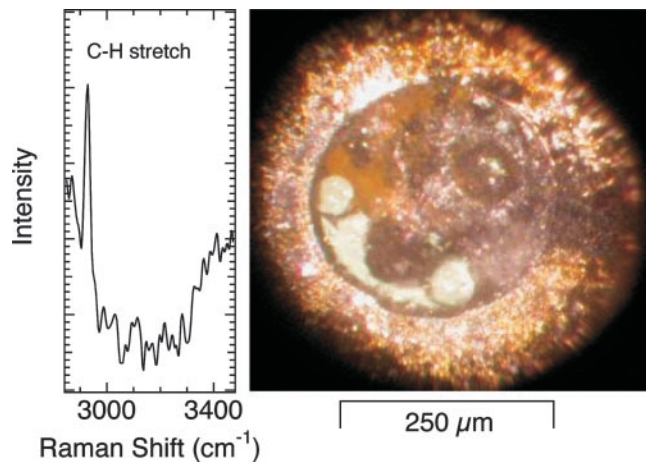


Fig. 3. Raman spectra (*Left*) of low-pressure bubbles (*Right*) formed upon decompression to ≈ 0.5 GPa at room temperature after laser heating to $\approx 1,500^\circ\text{C}$ at 5.7 GPa. Note the absence of O-H stretching vibrations because the bubble has displaced the surrounding H_2O . Bubbles are visible near the bottom, left side, and slightly right of center.

in the experiments to date, but dispersed throughout the sample chamber in low enough concentration that detection is difficult until the H_2O -ice melts and the two phases separate.

Further insight into the chemical processes involved in high-pressure methane production may be obtained by analysis of the thermochemistry. Our aim is to address the temperature and pressure dependence of the methane-forming reaction; specifically, it is useful to determine whether the high-pressure formation of methane is indeed favored at lower temperatures, or the extent to which this is favored by resistive versus laser heating. In the resistive heating experiments, a hot fluid phase is allowed to be in contact with the steel gasket containing the sample; thus catalytic activity of the gasket is possible (e.g., ref. 5). In contrast, the heated area is localized in laser heating experiments such that the material near the gasket remains subsolidus (e.g., ice). High-pressure chemical equilibrium was calculated with the Cheetah (22) thermochemical code. The calculations used a single fluid phase of variable chemical composition in equilibrium with several solid phases. Species in the fluid phase were treated with a spherical exponential-6 fluid model; solid phases were treated with simple or extended Murnaghan equations of state (23). Note that the scaled particle theory/simplified perturbed hard-chain theory calculations of Kenney *et al.* (6) do not consider solid phases and have a more limited pressure range than the Cheetah code.

The following species were considered for the fluid phase: C, H, H_2 , O, O_2 , O_3 , Fe, Ca, CaO, CH_4 , C_2H_6 , C_2H_4 , C_2H_2 , H_2O , CO, CO_2 , CH_3OH , and $\text{C}_2\text{H}_5\text{OH}$. The following solid species were considered for the condensed phases: Ca(I), Ca(II), CaO(B1), CaO(B2), CaCO_3 (calcite), CaCO_3 (aragonite), C(diamond), C(graphite), Fe, FeO(B1), Fe_2O_3 , Fe_2O_3 (II), Fe_3O_4 (magnetite), and Fe_3O_4 (h-phase). Several liquid phase species, Ca, Fe, C, FeO, CaCO_3 , and CaO, were also considered in the calculations. Our calculations assumed full chemical equilibrium (i.e., representing a hypothetical experiment conducted for an infinite amount of time). Chemical equilibrium calculations are appropriate to the high-temperature experiments reported here, where most reactions are assumed to be fast compared to the time scale of the experiment.

Fig. 4 shows the concentration of species for an 8:1:20 molar ratio of FeO, CaCO_3 , and H_2O at 500°C . Hydrocarbons were found for pressures < 8 GPa. This finding suggests that the experimental weakness of the Raman signature of methane at

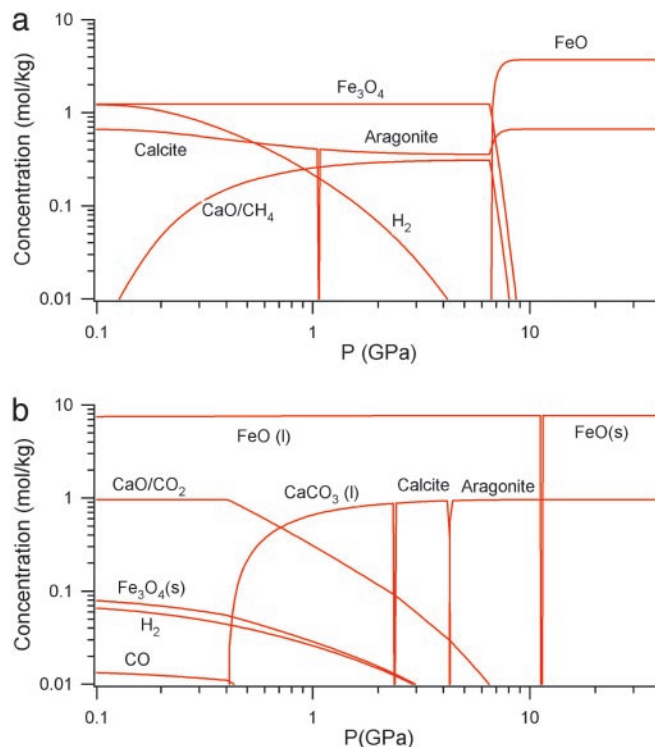
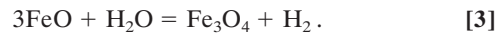


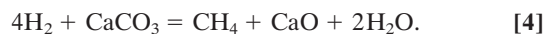
Fig. 4. Results of thermochemical calculations. Concentrations at 500°C (a) and $1,500^\circ\text{C}$ (b). CH_4 is predicted to be prevalent at 500°C above 0.9 GPa, as shown in a, but H_2 becomes dominant at $1,500^\circ\text{C}$, as shown in b. Concentrations are shown per kg of $\text{H}_2\text{O}/\text{CaCO}_3/\text{FeO}$ mixture. Liquid phases are denoted by (l), and solid phases are denoted by (s). Lines representing more than one species are labeled with a /.

high pressure is caused by a shifting chemical equilibrium, in addition to the phase separation observed. The only hydrocarbon species with significant concentration is CH_4 . Its concentration is substantial for pressures up to 2 GPa. Molecular hydrogen is predicted to accompany CH_4 . Hydrogen dominates at low pressures, whereas the hydrogen and CH_4 concentrations become comparable at pressures > 1 GPa. Hydrogen is formed in our calculations from the breakdown of FeO:



The varying H_2 concentrations shown in Fig. 4 are caused mostly by the equilibrium of reaction 3. In calculations of a 4:10 molar mixture of FeO/water at 500°C , we found that decomposition is nearly complete at low pressures, whereas at pressures > 5 GPa almost no decomposition (and concomitant production of hydrogen) was found. Although we have not detected H_2 experimentally, it may be dispersed at a concentration below our detection limit, or it may react with and enter the gasket material.

The calculations predicted that the concentrations of CaO and CH_4 were nearly equal at 500°C , suggesting the following decomposition mechanism for CaCO_3 :



Carbon in the form of graphite or diamond is not predicted to form at 500°C at any pressure considered. Calcite is predicted to convert to aragonite at pressures > 1 GPa. Aragonite and FeO are predicted to be stable until decomposition at pressures > 7 GPa. Our calculations show that methane production is disfavored at higher temperatures. Fig. 4b shows the concentration of species for the mixture at $1,500^\circ\text{C}$. In this case the CaO con-

centration was found to be nearly equal to the CO₂ concentration. This finding is in contrast to the calculation at 500°C, where the CO₂ concentration was negligible. The results indicate the following decomposition mechanism:



If we subtract the high-temperature mechanism (5) from the low-temperature mechanism (4), we are left with the well known methane reforming reaction:



Significant quantities of CO associated with partial oxidation in the reforming reaction are also found at higher temperatures as shown in Fig. 4b. High temperatures favor H₂ and CO₂, whereas lower temperatures favor CH₄ and H₂O. In calculations of a 10% molar ratio of H₂O to CO₂, we found that methane formation is favored under 1,200°C at 1 GPa, whereas H₂ formation was favored over 1,200°C. In Fig. 4b the concentrations of magnetite and H₂ are nearly equal at 1,500°C, indicating the dominance of reaction 3.

Chemical equilibrium calculations on a representative 1:10 molar mixture of CH₄ and H₂O were also performed with the CHEQ thermochemical code (24) to determine whether fluid-fluid phase separation is thermodynamically favored at the experimental conditions. The CHEQ code does not include the solid phases considered in the Cheetah modeling, but has the ability to determine chemical equilibrium between several mixed fluid phases. The major fluid species allowed were the same as in the Cheetah code. The results indicate that a separation into CH₄-rich and H₂O-rich phases should be favored at all pressures for temperatures <≈700°C, whereas at 1,500°C pressures of >≈23 GPa are predicted to be necessary to induce phase separation. These results are in agreement with the formation of methane bubbles that we observed upon decompression and cooling to room temperature of the diamond anvil cell.

Discussion

We report *in situ* observations of methane-forming reactions from a model mineral assemblage at the pressures and temperatures of the Earth's upper mantle. The results of our *in situ* experiments and thermochemical modeling differ markedly from those obtained by quenching (6), which found the yield of methane at 4 GPa from FeO + CaCO₃ + H₂O was very small at 600°C and below but climbed steadily up to 1,200°C. The

previous thermochemical calculations (6) do not pertain to this experimental reactant mixture but rather treat the formation of higher hydrocarbons from an assumed supply of methane.

Methane is expected to form inorganically at mantle pressures and temperatures from any carbonate species, such as FeCO₃-siderite or MgCO₃-magnesite, in the presence of H₂O at oxygen fugacities near the wüstite-magnetite fO₂ buffer. Such conditions may be widespread in the mantle and can be moderated by the presence of iron-bearing phases such as Fe₂SiO₄-fayalite, FeS-troilite, or accessory minerals such as FeCr₂O₄-chromite and FeTiO₃-ilmenite. Indeed, our analysis shows that methane production is thermodynamically favorable under a broad range of high pressure-temperature conditions. The calculations indicate that methane production is most favored at 500°C and pressures <7 GPa; higher temperatures are expected to lead to CO₂ and CO production through a reforming equilibrium with methane. The wide pressure-temperature-composition stability field of methane documented here has broad implications for the hydrocarbon budget of the planet and indicates that methane may be a more prevalent carbon-bearing phase in the mantle than previously thought, with implications for the deep hot biosphere (25). In particular, isotopic evidence indicating the prevalence of biogenic hydrocarbons pertains to economically exploited hydrocarbon gas reservoirs, largely in sedimentary basins (2); these observations and analyses do not rule out the potential for large abiogenic reservoirs in the mantle. Moreover, the assumption that CO₂ is the sole carrier of mantle-derived noble gases (26, 27) should be reevaluated. Finally, the potential may exist for the high-pressure formation of heavier hydrocarbons by using mantle-generated methane as a precursor.

We thank I. M. Chou, F. Dyson, G. D. Cody, S. A. Gramsch, R. M. Hazen, J. Katz, and B. Sherwood Lollar for critical comments; and D. Errandonea, M. Frank, D. Frost, M. Furlanetto, J. Katz, J. Lin, B. Mysen, M. Phillips, S. A. Schellenberg, V. V. Struzhkin, and O. L. Tschauer for technical assistance and helpful discussions. This research is supported by the National Science Foundation, National Aeronautics and Space Administration Astrobiology Institute under Cooperative Agreement NNA04C09A, and the National Science Foundation and Department of Energy/National Nuclear Security Administration through the Carnegie/Department of Energy Alliance Center (Grant DE-FC03-03NA00144). The Advanced Photon Source is supported by the U.S. Department of Energy, Basic Energy Sciences, Office of Energy Research, under Contract W-31-109-Eng-38. D.R.H. acknowledges support through a Green Fellowship of the Carnegie Institution, and H.P.S. is currently supported by an Indiana University-South Bend Faculty Research Grant.

1. Sherwood Lollar, B., Frapé, S. K., Weise, S. M., Fritz, P., Macko, S. A. & Welhan, J. A. (1993) *Geochim. Cosmochim. Acta* **57**, 5087–5097.
2. Sherwood Lollar, B., Westgate, T. D., Ward, J. A., Slater, G. F. & Lacrampe-Couloume, G. (2002) *Nature* **416**, 522–524.
3. Horita, J. & Berndt, M. E. (1999) *Science* **285**, 1055–1057.
4. Foustoukos, D. I. & Seyfried, W. E. (2004) *Science* **304**, 1002–1005.
5. McCollom, T. M. & Seewald, J. S. (2003) *Geochim. Cosmochim. Acta* **67**, 3625–3644.
6. Kenney, J. F., Kutcherov, V. A., Bendeliani, N. A. & Alekseev, V. A. (2002) *Proc. Natl. Acad. Sci. USA* **99**, 10976–10981.
7. Holloway, J. R. (1984) *Geology* **12**, 455–458.
8. French, B. M. (1966) *Rev. Geophys.* **4**, 223–253.
9. Huizenga, J. M. (2001) *Lithos* **55**, 101–114.
10. Shock, E. L. & Helgeson, H. C. (1990) *Geochim. Cosmochim. Acta* **54**, 915–945.
11. McCollom, T. M. (2003) *Geochim. Cosmochim. Acta* **67**, 311–317.
12. Duan, Z., Möller, N. & Weare, J. H. (2000) *Geochim. Cosmochim. Acta* **64**, 1069–1075.
13. Frost, D. J. & Wood, B. J. (1995) *Contrib. Mineral. Petrol.* **121**, 303–308.
14. Egger, D. H. & Baker, D. R. (1982) in *High-Pressure Research in Geophysics (Advances in Earth and Planetary Sciences)*, eds. Akimoto, S. & Manghnani, H. M. (Centre for Academic Publishing, Tokyo), Vol. 12, pp. 237–250.
15. Jakobsson, S. & Holloway, J. R. (1986) *J. Volcanol. Geotherm. Res.* **29**, 265–291.
16. Bassett, W. A., Shen, A. H., Bucknum, M. & Chou, I. M. (1993) *Rev. Sci. Instrum.* **64**, 2340–2345.
17. Ma, Y., Mao, H. K., Hemley, R. J., Gramsch, S. A., Shen, G. Y. & Somayazulu, M. (2001) *Rev. Sci. Instrum.* **72**, 1302–1305.
18. Tschauer, O., Mao, H. K. & Hemley, R. J. (2001) *Phys. Rev. Lett.* **87**, 075701.
19. Mao, H. K., Bell, P. M., Shaner, J. W. & Steinberg, D. J. (1978) *J. Appl. Phys.* **49**, 3276–3283.
20. Hebert, P., Polian, A., Loubeyre, P. & Le Toullec, R. (1987) *Phys. Rev. B* **36**, 9196–9201.
21. Walrafen, G. A., Abebe, M., Mauer, F. A., Block, S. & Piermarini, G. J. (1982) *J. Chem. Phys.* **77**, 2166–2174.
22. Fried, L. E. & Howard, W. M. (1999) *J. Chem. Phys.* **110**, 12023–12032.
23. Fried, L. E. & Howard, W. M. (2000) *Phys. Rev. B* **61**, 8734–8742.
24. Ree, F. H. (1984) *J. Chem. Phys.* **81**, 1251–1263.
25. Gold, T. (1999) *The Deep Hot Biosphere* (Copernicus, New York).
26. Sherwood Lollar, B., Ballentine, C. J. & O'Nions, R. K. (1997) *Geochim. Cosmochim. Acta* **61**, 2295–2307.
27. Ballentine, C. J., Schoell, M., Coleman, D. & Cain, B. A. (2001) *Nature* **409**, 327–331.